

E7-2002-237

S. M. Lukyanov\*, Yu. E. Penionzhkevich

**PECULIARITIES OF O–Mg ISOTOPES  
AT THE NEUTRON DRIP LINE**

Submitted to «52nd Meeting on Nuclear Spectroscopy  
and Nuclear Structure (NUCLEUS-2002)»,  
June 18, 2002, Moscow, Russia

---

E-mail: [lukyanov@flnr.jinr.ru](mailto:lukyanov@flnr.jinr.ru)

The study of the properties of neutron-rich nuclei far from stability is one of the most exciting areas of modern research in nuclear physics. The progress in our knowledge of the properties of these nuclei has enormously broadened because of the new radioactive ion beam facilities and the development of very sophisticated fragment separators.

One interesting feature has been found in the region of the light neutron-rich nuclei. As it was established in 1975 by C.Thibault et al. [1], neutron rich nuclei with  $N \approx 20$  constitute a good example of shape coexistence of spherical and deformed configurations (for example,  $^{32}\text{Mg}$ ). In the frame of the shell model, the deformed ground state in  $^{32}\text{Mg}$  is a consequence of the strong correlation energy of  $2p-2h$  neutron excitations from the  $sd$ - to the  $pf$ -shell. It was suggested that the extra binding energy was gained by the deformation associated with the particle-hole excitation across the  $N=20$  shell gap. If a nucleus gains binding energy through deformation, the drip line extends further than expected for a closed shell. Recent experiments at GANIL and RIKEN were dedicated to the study of the stability of the neutron-rich nuclei with  $Z > 7$  and around  $N = 20$ . The variation of the shell gap and deformation as a function of  $N$  and  $Z$  could be a major challenge.

Modern radioactive nuclear beam facilities allow to produce and study intense beams of very neutron-rich nuclei, previously unavailable. The aim of the experiments was to study the particle stability of these nuclei, their masses, which constitute the basic knowledge of the nucleus, and their spectroscopic characteristics.

### **Particle stability of neutron-rich nuclei at and around double magicity $N=20$ and $N=28$**

Among the recent experiments dedicated to explore the neutron drip line in the region of elements from O to Mg one could mention those on the particle instability of the neutron rich oxygen isotopes  $^{26,28}\text{O}$  [2-4] and on the discovery of the particle stability of  $^{31}\text{Ne}$  [5] and  $^{31}\text{F}$  [6]. The appearance of a so-called "island of inversion" with respect to the particle stability of isotopes has been claimed through various theoretical predictions. A particular feature in this region is the progressive development of a deformation in spite of the expected effect of spherical stability due to the magicity of the neutron number  $N=20$  [7-10]. It was argued that the deformation might lead to enhanced binding energies in some of yet undiscovered neutron-rich nuclei.

The question of the possible stability of the double magic nucleus  $^{28}\text{O}$ , had recently attracted much attention, even though the particle instability of  $^{25,26}\text{O}$  beyond  $^{24}\text{O}$  has been clearly shown by the experiments [2]. The expectation for  $^{28}\text{O}$  to be stable stems from an enhanced stability anticipated from the double magicity or the deformation. The stability of  $^{28}\text{O}$  has been

discussed in several theoretical papers, which however yielded conflicting results. Recently, an attempt to search for  $^{28}\text{O}$  has been made by using a  $^{36}\text{S}$  beam [3]. No events of  $^{28}\text{O}$  were observed, and the particle instability of  $^{28}\text{O}$  was concluded from a comparison with the larger estimated yield in the case of particle bound character of  $^{28}\text{O}$ . Such yield estimate was made by means of an extrapolation method using the results of heavier isotones of  $N=20$ . This extrapolation may, however, involve some ambiguities since the  $Z, A$  dependence of the production cross sections is not well understood theoretically. In order to reduce possible uncertainty, use of an interpolation method, which was once applied for the first evidence for the instability of  $^{26}\text{O}$ , should be desirable.

The puzzle of the instability of double magic nuclide  $^{28}\text{O}$  become more intriguingness regarding the next performed experiments. The recent discoveries of the particle stability of  $^{31}\text{Ne}$  [5] and  $^{31}\text{F}$  [6], in contrast to most of mass predictions, have motivated us to re-examine the location of the fluorine drip line. The production cross section of  $^{31}\text{F}$  was then obtained to be about  $0.15 \pm 0.06$  pb. Two-dimensional  $A/Z$  versus  $Z$  plot is shown in Fig.1, which was obtained in the reaction of a  $94.1\text{A MeV } ^{40}\text{Ar}$  beam on a  $690 \text{ mg/cm}^2$  tantalum target during a 4-day run. A new isotope  $^{31}\text{F}$  is clearly visible (8 events). No events associated with  $^{25}\text{N}$  and  $^{28}\text{O}$  as well as  $^{24}\text{N}$ ,  $^{25,26,27}\text{O}$  and  $^{30}\text{F}$  were obtained. In the case of the particle stability of  $^{28}\text{O}$  or  $^{25}\text{N}$ , the associate events are expected to appear inside the ellipses. The dashed lines are drawn guides to the eye for the isotopes with the same neutron numbers,  $N=2Z+2$  and  $N=2Z+4$ . The absence of events corresponding to the  $^{25,26,27,28}\text{O}$  isotopes as well as  $^{24,25}\text{N}$  and  $^{30}\text{F}$  is clearly confirmed. For instance, in the case of the particle stability of  $^{28}\text{O}$  or  $^{25}\text{N}$ , the associate events are expected to appear inside the ellipses in Fig.1, while no events were found in those domains.

The particle stability of  $^{31}\text{F}$  gives strong evidence on the onset of deformation in the region. One may underline that the drip line for the fluorine-magnesium elements could move far beyond the presently known boundaries.

The drip line for C, N and O isotopes is consistent with the closure of the  $\nu 2s_{1/2}$  orbital (as it is shown in Table). Particle instability of  $^{26,28}\text{O}$  isotopes indicates that the  $\nu 1d_{3/2}$  orbital energy is not low enough to bound nuclei. The additional proton makes the neutron potential deeper. For the fluorine isotopes neutrons can fill completely the  $1d_{3/2}$  orbital for  $^{29}\text{F}$ , and the  $1f_{7/2}$  orbital starts to fill in  $^{31}\text{F}$ .

Therefore, there is a great interest to study nuclei in the region of the neutron closure  $N=28$ . Experimentally, the properties of  $^{44}\text{S}$  have been studied and it was concluded that the

ground state of  $^{44}\text{S}$  is deformed. This result suggested a significant breaking of the  $N=28$  closure for nuclei near  $^{44}\text{S}$ .

We present the modern results of our attempt to determine the neutron drip line for the Ne-Mg isotopes in the region of the neutron numbers  $N = 20-28$ . In particular, our experiment was dedicated to the direct observation of the  $^{31}\text{F}$ ,  $^{34}\text{Ne}$ ,  $^{37}\text{Na}$  and  $^{40}\text{Mg}$  nuclei. These nuclei were searched for among the fragmentation products of a 59.8 AMeV  $^{48}\text{Ca}$  beam on a 160  $\mu\text{m}$  tantalum target. The very neutron rich beam and target were chosen to optimize the production rate of the drip-line nuclei in accordance with the LISE code [11,12] and the results of the previous work [13]. The mean intensity of the  $^{48}\text{Ca}$  beam was 150 pA. The experiment benefited of a recent update of the LISE [14] spectrometer to the LISE 2000 [15] level. The upgrade includes: an increase of the maximum magnetic rigidity to 4.3 Tm, an increase by a factor of 2.5 of the angular acceptance and a new line with improved optics. As a consequence, a total increase of a factor 10 in the production rate of the drip-line nuclei has been achieved with respect to using the standard LISE spectrometer.

The reaction fragments were collected and analyzed by the LISE 2000 spectrometer operated in an achromatic mode and at the maximum values of momentum acceptance (5%) and solid angle (1.9 msr). The magnetic rigidity of the first and the second half of the spectrometer was set at 3.48 Tm and 3.391 Tm, respectively. To reduce the overall counting rate due to light isotopes a beryllium wedge with a mean thickness of 563  $\text{mg}/\text{cm}^2$  was placed at the momentum dispersive focal plane.

In addition to the standard identification method of the fragments via time-of-flight (ToF), energy loss (dE) and total kinetic energy (TKE), a multiwire proportional detector was placed in the dispersive plane of the LISE 2000 spectrometer. This detector allowed measuring the magnetic rigidity of each fragment via its position in the focal plane, improving the mass to charge resolution ( $A/Q$ ). The sensitive area of this detector was 10cm(H)x5cm(V), covering the full momentum acceptance of the spectrometer. The cathode wires were individually read out. A spatial resolution of 0.5 mm was achieved for a counting rate of  $10^4$  particles per second. The typical efficiency for this particle detector was about 80%. The mass-to-charge ratio ( $A/Q$ ) was obtained with an accuracy of 0.8%. The selected fragments were implanted in a telescope consisting of seven silicon detectors for the identification of the fragments. In the data analysis, the fully stripped fragments were selected by putting gates on the total kinetic energy measured with the silicon telescope.

The result of the particle identification based only on the dE, ToF, and TKE is shown in Fig. 2a, where the energy loss measured in the first detector of the telescope is plotted versus the

time of flight (ToF) between the dE silicon telescope and the cyclotron radiofrequency. This matrix was obtained from the data accumulated during 2.5 days with a mean intensity of the primary beam of 150 pA. The new isotopes  $^{34}\text{Ne}$  (two events) and  $^{37}\text{Na}$  (one event) are clearly visible. The discovery of  $^{31}\text{F}$  [6] is also confirmed. The  $^{34}\text{Ne}$  and  $^{37}\text{Na}$  isotopes have also been unambiguously identified by using the calculated value of  $A/Z$ . This value was obtained from the ToF and from  $B_p$ , measured by means of the multiwire detector. The two-dimensional  $A/Z$  vs.  $Z$  plot is shown in Fig. 2b. The presence of the events corresponding to  $^{34}\text{Ne}$  and  $^{37}\text{Na}$  confirms that these nuclei are bound. The one event of  $^{34}\text{Ne}$  is absent in Fig. 2b due to the fact that the efficiency of the multiwire detector is only 80% for light fragments. No events, which could be attributed to  $^{33}\text{Ne}$ ,  $^{36}\text{Na}$  and  $^{40}\text{Mg}$ , were observed.

Yields of  $N=2Z$ ,  $N=2Z+2$  and  $N=2Z+4$  nuclei versus the  $Z$ -value are shown in Fig. 3. The yield estimations for the fragments were calculated according to the LISE-code [12]. An attempt to describe the experimental distributions of the fragments was undertaken by convolution of Gaussian form of the beam velocity and of an exponential tail at lower energies.

The experimental data were fitted by the same value of  $\sigma = 107$  MeV/c (the parameter of the momentum distribution in the convolution [12]) for the three different cases  $N=2Z$ ,  $N=2Z+2$  and  $N=2Z+4$ . For nuclei with  $N=2Z$  and  $N=2Z+2$  we found an agreement between the experimental and calculated values. The calculated values for the nuclei with  $N=2Z+4$  is higher than the experimental ones for  $Z$  greater than 6.

The most interesting nuclide in this region is  $^{40}\text{Mg}$ , which is probably not bound since no counts have been observed. We estimated the upper limit for the production cross section of  $^{40}\text{Mg}$  to be less than 0.06 pb. However, the present results do not allow drawing a definite conclusion on the instability of  $^{40}\text{Mg}$ ; this is also supported by the trend of the calculated yield in Fig. 3. The production cross section for  $^{34}\text{Ne}$  and  $^{37}\text{Na}$  was estimated to be about  $0.17 \pm 0.12$  pb and  $0.06 \pm 0.06$  pb, respectively. The cross section for  $^{31}\text{F}$  is estimated to be about 0.7 pb. This value for the production of  $^{31}\text{F}$  in the reaction  $59.8\text{AMEV } 48\text{Ca} + \text{natTa}$  is about 5 times higher than in the reaction  $94.1\text{AMEV } ^{40}\text{Ar} + \text{Ta}$  [6].

From the theoretical point of view, the description of the light nuclei in the *sd-pf* shells is still a problem. In particular, the calculation of the binding energy for the very neutron rich isotopes of O, F, Ne and Na is a real challenge. There are various theoretical calculations (viz., the finite-range liquid drop model (FRLD) [16], two versions of the shell model (SM) [17-19], the relativistic mean field theory [20] and the Hartree-Fock model [21]), which predict the position of the neutron drip line in this region. For instance, the FRLD model gives a very strong binding energy for  $^{40}\text{Mg}$ . In the frame of this model one- and two-neutron separation energies are even

above 3.4MeV. One may note that the FRLD model gives correct predictions for the stability of  $^{31}\text{Ne}$  and  $^{31}\text{F}$ , implying nuclear deformation effects for both the macroscopic and microscopic parts. According to the shell model predictions [18], the last bound isotopes are  $^{24}\text{O}$ ,  $^{27}\text{F}$ ,  $^{34}\text{Ne}$ ,  $^{37}\text{Na}$ ,  $^{38}\text{Mg}$  and  $^{43}\text{Al}$ . However, slight changes of the drip line cannot be excluded since  $^{37}\text{Na}$  was predicted to be bound only by 250 keV, while  $^{31}\text{F}$ ,  $^{40}\text{Mg}$  and  $^{43}\text{Al}$  are unbound by 145, 470 and 550 keV, respectively. According to another shell model calculation [17]  $^{26}\text{O}$ ,  $^{34}\text{Ne}$  and  $^{40}\text{Mg}$  are the last stable isotopes against two-neutron emission, as indicated by their maximal binding energy. Both SM and HF calculations for even-mass O, Ne and Mg indicate a disappearance of shell magic numbers, and suggest an onset of deformation and a shape coexistence in this region.

The stability/instability of the present nuclei can be explained by taking into account various degrees of mixing in the *sd* and *fp* shells, which are related to the deformation effects. According to our results, the neutron drip line is extended beyond N=20 and reaches N=24 for neon and even N=26 for sodium isotopes as a consequence of the mixing of the  $d_{3/2}$  and  $f_{7/2}$  states, while the N=20 shell closure disappears.

In summary, the neutron-rich isotopes  $^{34}\text{Ne}$  and  $^{37}\text{Na}$  were observed using the newly upgraded LISE 2000 spectrometer and the reaction  $^{48}\text{Ca}+^{nat}\text{Ta}$  at 59.8 AMeV. Thus, most probably, the neutron drip line has been reached for the neon and sodium isotopes. However, it seems that to definitely conclude whether these isotopes do mark the drip line or do not will need to perform further experimental efforts.

### **Mass measurement of heavy isotopes from Ne up to Ar**

The question of particle stability is directly related to the masses and nuclear binding energies, which are very sensitive to the existence of shells and may provide clear signatures of shell closures.

An experiment on mass measurement using a direct time of flight technique was undertaken [22] in order to investigate the N=20 and N=28 shell closures for nuclei from Ne (Z=10) to Ar (Z=18) and thus to bring some clarifications concerning the behaviour of magic numbers far from stability. The nuclei of interest were produced by the fragmentation of an E/A=60 MeV  $^{48}\text{Ca}$  beam on a Ta target located in the SISSI device of the accelerator complex at GANIL.

The two-neutron separation energies  $S_{2n}$  derived from the measured masses are displayed in Fig.4. Such systematics are of particular interest as the  $S_{2n}$  values correspond to a "derivative" of the mass surface. The new data are presented with error bars while the others, except the encircled data, are taken from Audi and Wapstra. The Ca, K and Ar isotopes show a

behaviour typical of the filling of shells, with the two shell closures at  $N=20$  and  $N=28$  being evident at the corresponding sharp decrease of the  $S_{2n}$  for the next two isotopes and a moderate decrease of  $S_{2n}$  for subsequent points as the filling of the next shell starts to influence  $S_{2n}$ . The sharp drop at  $N=22$ , shown by the dashed vertical line and corresponding to the shell  $N=20$  is clearly visible through all the Si-Ca region, while going to lower  $Z$  to the Al-Na region this drop seems to move towards lower  $N$ .

This was the reason why we made an attempt to clarify the situation of two-neutron separation energies in this region.  $S_{2n}$  values must be positive and therefore, we included the "expected"  $S_{2n}$  values of the heaviest particle stable isotopes  $^{23}\text{N}$ ,  $^{22}\text{C}$  and  $^{29,31}\text{F}$  to the graph, they are marked by circles. The "expected"  $S_{2n}$  values for  $^{29,31}\text{F}$  point out the region where they probably have to be located due to their experimentally found particle stability (positive  $S_{2n}$  values). Their values have been tentatively estimated as a half of the  $S_{2n}$  value of preceding particle stable isotope to ensure the most probable decrease of  $S_{2n}$  values. The "expected"  $S_{2n}$  values of the heaviest particle stable isotopes  $^{23}\text{N}$  and  $^{22}\text{C}$  have been placed in the plot to follow the trend seen in oxygen isotopes with  $N > 14$ .

These values are not crucial for determination of the shell closure at  $N=16$ , important is only the fact that particle stable isotopes heavier than  $^{23}\text{N}$  and  $^{22}\text{C}$  do not exist. The inclusion of the  $S_{2n}$  values for  $^{29}\text{F}$  and  $^{31}\text{F}$  was most important, because this allowed us to observe the sharp drop of  $^{27}\text{F}$  value followed by a moderate decrease of  $S_{2n}$  values for  $^{29}\text{F}$  and  $^{31}\text{F}$  giving a very clear evidence for the existence of the new shell closure at  $N=16$  for fluorine. A similar behaviour confirming the  $N=16$  shell closure can be seen at the neon isotopes that exhibit a moderate decrease of  $S_{2n}$  values for  $^{29}\text{Ne}$  and  $^{30}\text{Ne}$ . We have already mentioned that in the Al-Na region the sharp drop in  $S_{2n}$  values.

It should be noted that the evidence for a new magic number  $N=16$  [23] follows also from Fig.4 where the  $S_{2n}$  values are plotted versus atomic number  $Z$ . The position of various possible shells or pseudo-shells are also shown in the figure. The shells  $N=20$  and  $28$  appearing in Fig.4. As has been already pointed out by the Cl, S and P isotopes exhibit a pronounced change of slope around  $N=26$ . Moreover, this change in the Cl and S isotopes is confirmed by the sharp drop at  $N=28$ .

The discontinuity observed at  $N=26$  [24] can now be understood in a simple Nilsson picture. For a prolate deformation of  $\beta \sim 0.2$ , a large gap appears between the lowest three orbits and the fourth orbital arising from the  $1f_{7/2}$  and higher orbitals. Consequently, a pseudo shell-closure can be considered to appear at  $N=26$ . Oblate deformations would not be compatible with these observations. Consequently, a pseudo-shell closure can be considered

to appear at  $N=26$ . As can be seen in Fig. 4 interesting new results have been also obtained for the Ne to Al isotopes. In particular, the steep decrease of the  $S_{2n}$  for  $^{35,36}\text{Mg}$  suggests that the Mg isotopes may become unbound at much lower neutron number than the predicted value of  $N=28$ . However, further experimental and theoretical work is required to confirm this conjecture.

### Gamma-ray energy of the first $2^+$ level for even-even nuclei.

Since the spectroscopic measurements can reveal details of the underlying microscopic structures, the in-beam  $\gamma$ -ray spectroscopy is an effective tool to check for shell closures. The information on the energy of the first excited state and on the  $B(E2)(2^+ \rightarrow 0^+)$  represents only the first step to understand the structure and to estimate the deformation of the nucleus. Additional information on relative intensities and the  $E(4^+)/E(2^+)$  ratio is also highly desirable. Such a measurement can probe of the underlying microscopic structures, determine the shape of the nuclei under study and give a new information on gaps between neighbour orbitals. Recently, in-beam  $\gamma$ -ray spectroscopy measurements [23,24] of a large number of exotic nuclei produced by the fragmentation of  $^{36}\text{S}$  and  $^{48}\text{Ca}$  projectiles on a thin Be target were performed at GANIL. In the experiment the coincidences between the outgoing fragments collected and identified at the focal plane of SPEG spectrometer and  $\gamma$ -rays measured using the array of 74  $\text{BaF}_2$  and four Ge segmented clover detectors, covering roughly 80% of the solid angle around the target.

From intensity argument, the line at 3.1 MeV for the Doppler-corrected  $\gamma$ -decay spectra of  $^{22}\text{O}$ , observed for the first time [25] represents, the  $2^+ \rightarrow 0^+$  transition in  $^{22}\text{O}$  and thus extends the systematics of the first  $2^+$  state energies of oxygen isotopes up to  $N=14$ . The dependence of the gamma-ray energy of the first  $2^+$  excited state on neutron number for even-even nuclei is presented in Fig.5. It should be noted that oxygen isotopes exhibit the lowest  $E(2^+)$  energy of 1.7 MeV for  $^{20}\text{O}$ , i.e. near the half-occupancy of the  $d_{5/2}$  subshell ( $N=12$ ) just like the Ne and Mg isotopes do. However, the enhancement of  $E(2^+)$  energy at  $N=14$  for Ne and Mg is much smaller than that for oxygen. If the enhancement seen in oxygen also appears in carbon it will be another confirmation of the existence of  $N=16$  shell in the C-Ne region. Moreover, we should note that the non-existence of a bound excited state in  $N=16$  isotones of carbon and oxygen would also indicate the existence of shell at  $N=16$ .

As one can see in Fig.5, the energy of the first  $2^+$  state for Ne isotopes rises from 1.25 MeV for  $^{22}\text{Ne}$  to 2 MeV for  $^{24}\text{Ne}$  and  $^{26}\text{Ne}$  and then drops to 1.3 MeV for  $^{28}\text{Ne}$  showing the flat maximum for both 14 and 16 neutron numbers and suggesting a competition between the



$1d_{5/2}$  and  $2s_{1/2}$  orbits as well an elimination of the N=20 shell. On the other hand, Mg isotopes show a steady decrease in the energy of  $2^+$  state, confirming the weakening of N=20 shell after reaching the maximum at N=14.

In Fig.5 the  $\gamma$ -ray energies of the first  $2^+$  state for even isotopes of S, Ar and Ca are plotted. These nuclides exhibit pronounced maxima at N=20 shell, however, the strength of N=16 shell in these elements is very weak as these nuclides are no more neutron-rich but lie on the proton-rich side of the valley of  $\beta$ -stability.

So we can conclude, that the strength of N=20 and N=28 shells is variable in the region from carbon up to neon.

The authors would like to express their gratitude to the members of the FLNR (JINR, Dubna) – GANIL -Orsay-Dubna-Rez-Bucharest and FLNR (JINR, Dubna)-RIKEN(Japan) collaborations for the fruitful experimental efforts and discussions of the experimental results obtained in the joint experiments. This work has been carried out with financial support from PICS - (IN2P3) No. 1171, grant from INTAS 00-00463 and grant No. 96-02-17381a of the Russian Foundation for Basic Research.

Table

Nuclide p.b p.unbound	Proton configuration		Neutron Number	Neutron Configuration	
	bound	unbound		p.bound	unbound
<sup>19</sup> B	$\pi(1p_{3/2})^3$		14	$\nu(1d_{5/2})^6$	
<sup>22</sup> C	$\pi(1p_{3/2})^4$		16	$\nu(2s_{1/2})^2$	
<sup>23</sup> N	$\pi(1p_{1/2})^1$		16	$\nu(2s_{1/2})^2$	
<sup>25</sup> N		$\pi(1p_{1/2})^1$	18		$\nu(1d_{3/2})^2$
<sup>24</sup> O	$\pi(1p_{1/2})^2$		16	$\nu(2s_{1/2})^2$	
<sup>26</sup> O		$\pi(1p_{1/2})^2$	18		$\nu(1d_{3/2})^2$
<sup>28</sup> O		$\pi(1p_{1/2})^2$	20		$\nu(1d_{3/2})^4$
<sup>27</sup> F	$\pi(1d_{5/2})^1$		18	$\nu(1d_{3/2})^2$	
<sup>29</sup> F	$\pi(1d_{5/2})^1$		20	$\nu(1d_{3/2})^4$	
<sup>31</sup> F	$\pi(1d_{5/2})^1$		22	$\nu(1f_{7/2})^2$	
<sup>30</sup> Ne	$\pi(1d_{5/2})^2$		20	$\nu(1d_{3/2})^4$	
<sup>31</sup> Ne	$\pi(1d_{5/2})^2$		21	$\nu(1f_{7/2})^1$	
<sup>32</sup> Ne	$\pi(1d_{5/2})^2$		22	$\nu(1f_{7/2})^2$	

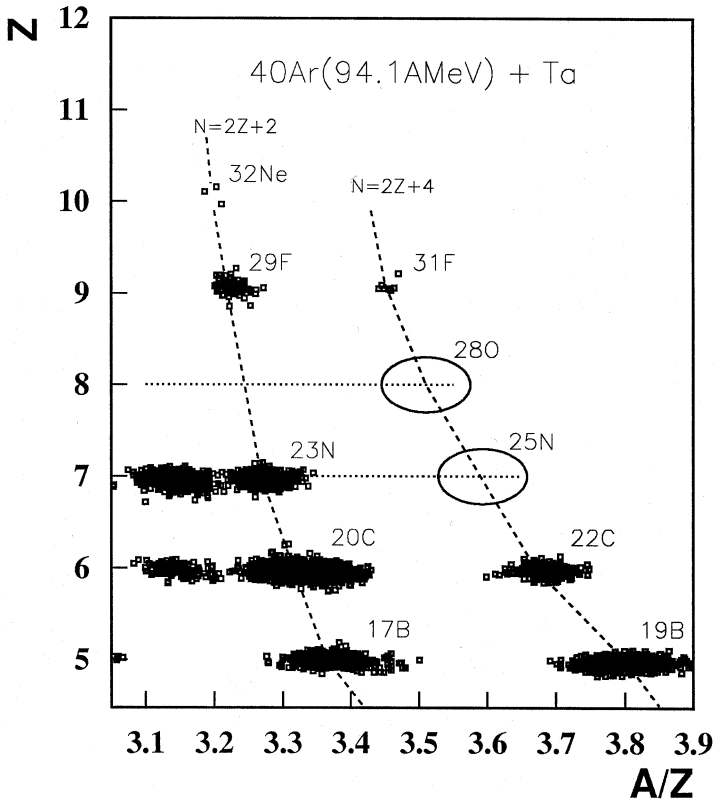


Fig.1

Two-dimensional A/Z versus Z plot, which was obtained in the reaction of a 94.1 AMeV  $^{40}\text{Ar}$  beam on a 690 mg/cm<sup>2</sup> tantalum target during a 4-day run. A new isotope  $^{31}\text{F}$  is clearly visible (8 events). No events associated with  $^{25}\text{N}$  and  $^{28}\text{O}$  as well as  $^{24}\text{N}$ ,  $^{25,26,27}\text{O}$  and  $^{30}\text{F}$  were obtained. In the case of the particle stability of  $^{28}\text{O}$  or  $^{25}\text{N}$ , the associate events are expected to appear inside the ellipses. The dashed lines are drawn guides to the eye for the isotopes with the same neutron numbers,  $N=2Z+2$  and  $N=2Z+4$ .

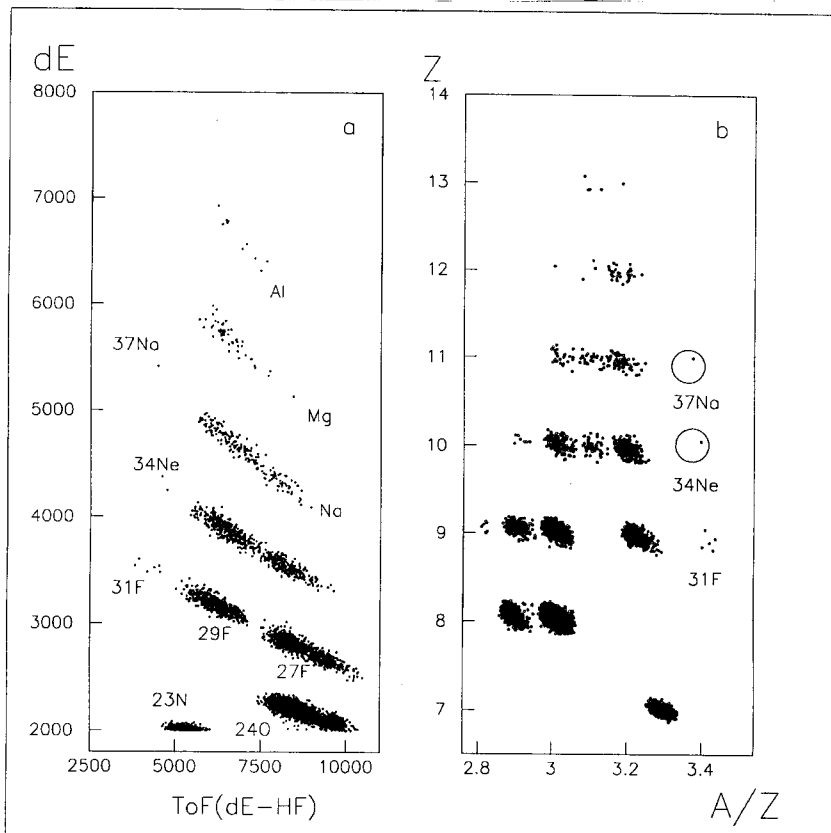


Fig.2

a) Energy-loss versus total-kinetic energy identification matrix.

b) Two-dimensional  $A/Z$  versus  $Z$  plot, which was obtained in the reaction of a  $58.9\text{A MeV } ^{48}\text{Ca}$  beam on a  $161\text{ mg/cm}^2$  tantalum target during a 2.5-days run. The new isotopes  $^{34}\text{Ne}$  (two events) and  $^{37}\text{Na}$  (one event) are clearly visible. No events associated with  $^{33}\text{Ne}$ ,  $^{36}\text{Na}$  and  $^{40}\text{Mg}$  were observed.

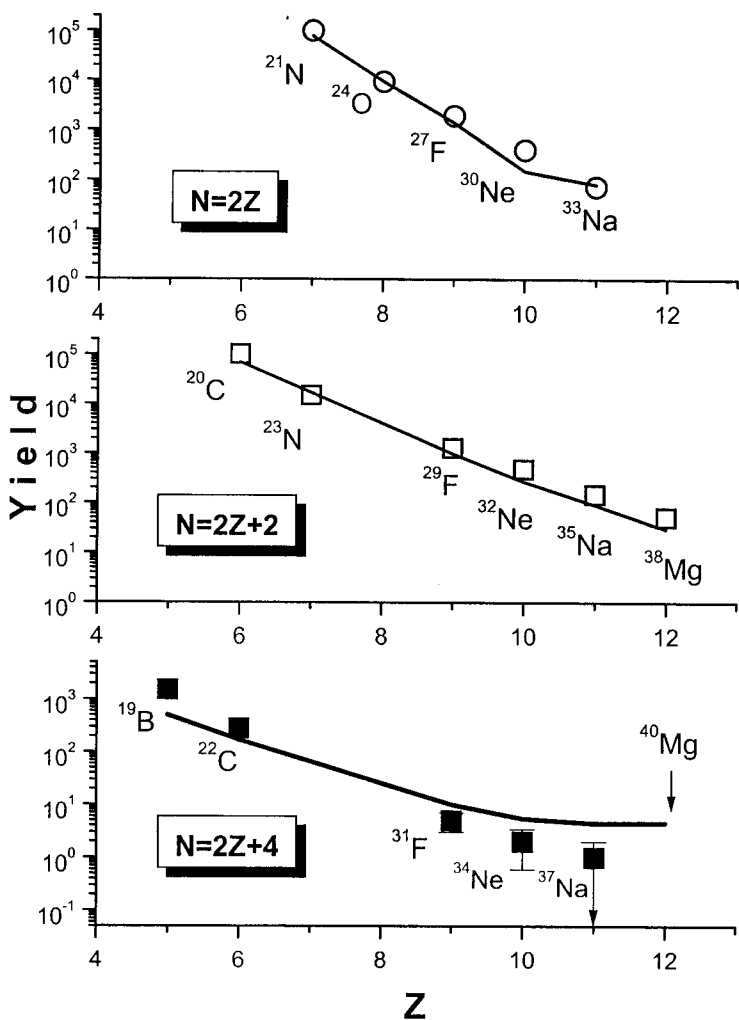


Fig.3  
 Isotopic production for nuclei with the neutron number  $N=2Z$ ,  $N=2Z+2$  and  $N=2Z+4$ . The solid lines present the expected yields according to the LISE-code.

# Mass measurement of heavy isotopes from Ne up to Ar

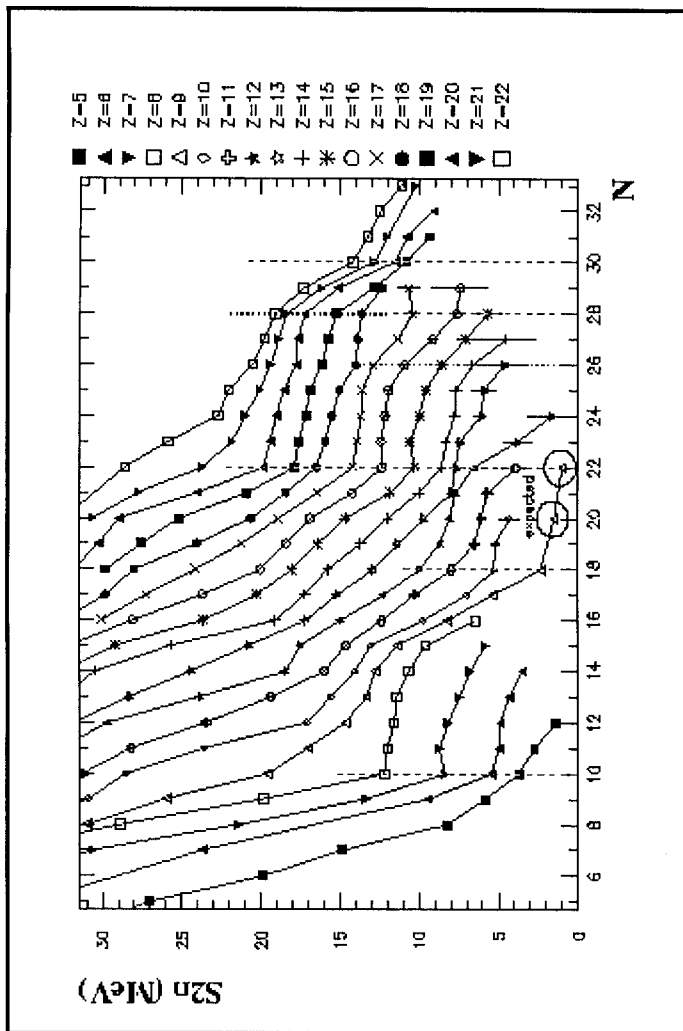


Fig.4

Two neutron separation energy  $S_{2n}$  versus neutron number for O-Ca isotopes.

# Gamma-ray energy of the first $2^+$ level for even-even nuclei.

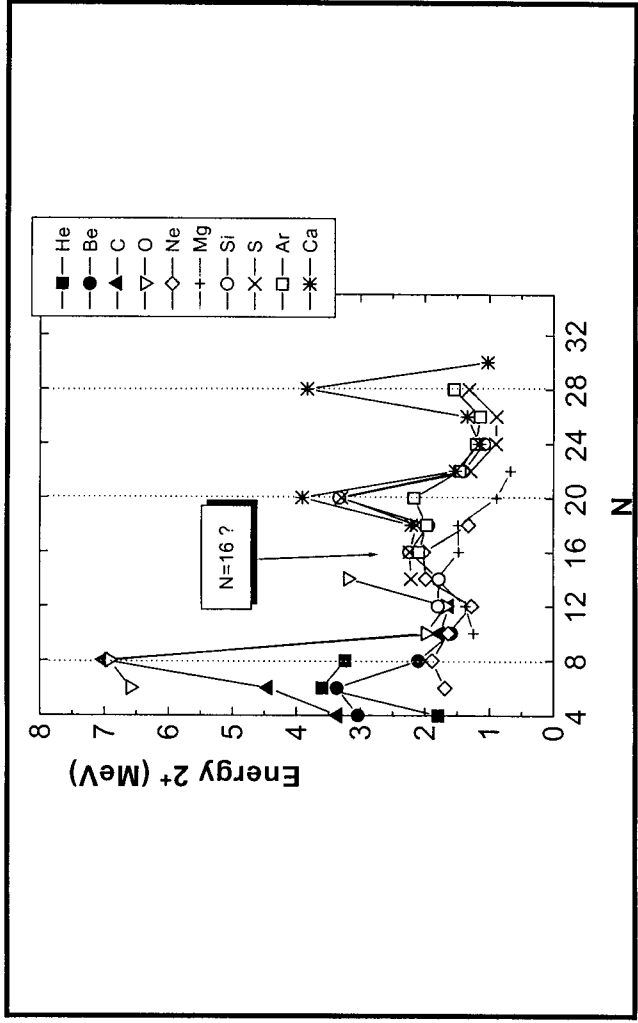


Fig.5  
The dependence of the gamma-ray energy of the first  $2^+$  excited state on neutron number for even-even nuclei.

### References:

1. C. Thibault *et al.*, Phys. Rev. C **12**, 644 (1975).
2. D. Guillemaud-Mueller *et al.*, Z. Phys. A**332**, 189 (1989).
3. O. B. Tarasov *et al.*, Phys. Lett. B **409**, 64 (1997).
4. M. Fauerbach *et al.*, Phys. Rev. C **53**, 47 (1996).
5. H. Sakurai *et al.*, Phys. Rev. C **54**, R2802 (1996).
6. H. Sakurai *et al.*, Phys. Lett. B **448**, 180 (1999).
7. X. Campi *et al.*, Nucl. Phys. A **251**, 193 (1975).
8. R. Nayak and L. Satpathy, Nucl. Phys. A **304**, 64 (1978).
9. A. Poves and J. Retamosa, Nucl. Phys. A **571**, 221 (1994).
10. E. K. Warburton, J. A. Becker and B. A. Brown, Phys. Rev. C **41**, 1147 (1990).
11. D. Bazin *et al.*, Nucl. Instr. and Meth. A **482**, 307 (2002).
12. <ftp://ftp.nsl.msui.edu/lise> or <http://www.nsl.msui.edu/lise>
13. O.B. Tarasov *et al.*, Nucl. Phys. A **629**, 605 (1998).
14. R. Anne *et al.*, Nucl. Instr. and Methods A **257**, 215 (1987).
15. R. Anne, Preprint GANIL, GANIL **P02 01** (2000).
16. P. Moller *et al.*, At.Data Nucl. Data Tables **39**, 185 (1995).
17. G. A. Lalazissis *et al.*, Phys. Rev. C **60**, 014310 (1999).
18. E. Caurier *et al.*, Phys. Rev. C **58**, 2033 (1998).
19. Y. Utsuno *et al.*, Phys. Rev. C **64**, 011301 (2001).
20. Z. Ren *et al.*, Phys. Rev. C **52**, R20 (1995).
21. J. Terasaki *et al.*, Nucl. Phys. A **621**, 706 (1997).
22. F. Sarazin *et al.*, Phys. Rev. Lett. **84** (2000) 5962.
23. Z. Dlouhy *et al.*, Nucl. Phys. A **701**, 189c (2002).
24. F. Azaiez, Phys.Scripta Vol. **T88** (2000) 118.
25. M. Belleguic *et al.*, Phys.Scripta Vol. **T88** (2000) 122.

---

Received on October 11, 2002.



## Особенности нейтронно-избыточных ядер в области O–Mg

Экспериментально исследована граница нейтронной стабильности в области от кислорода до магния. Для этого использовался фрагмент-сепаратор LISE (GANIL, Франция). Была выбрана реакция фрагментации ионов  $^{48}\text{Ca}$ . Новые нейтронно-избыточные изотопы  $^{34}\text{Ne}$  и  $^{37}\text{Na}$  были обнаружены как связанные ядра среди продуктов реакции фрагментации ионов  $^{48}\text{Ca}$ . Одновременно получены свидетельства, что  $^{33}\text{Ne}$  и  $^{36}\text{Na}$  являются несвязанными.

Приводятся также результаты экспериментов по измерению масс нейтронно-избыточных ядер. Анализ энергий связи, а также экспериментальный факт ядерной нестабильности дважды магической системы  $^{28}\text{O}$  указывают на изменение магических чисел для ядер с большим избытком нейтронов в области от углерода до кальция.

Важная информация о микроскопической структуре получена в результате последних экспериментов по измерению  $\gamma$ -спектроскопии в этой области ядер. Анализируются экспериментальные данные по измерению  $2^+$ -уровней для четно-четных ядер с числом нейтронов  $N=12-32$ .

Работа выполнена в Лаборатории ядерных реакций им. Г. Н. Флерова ОИЯИ.

Препринт Объединенного института ядерных исследований. Дубна, 2002

## Peculiarities of O–Mg Isotopes at the Neutron Drip Line

The neutron drip line in the oxygen–magnesium region has been explored by the projectile fragmentation of a  $^{48}\text{Ca}$  beam using the fragment separator LISe at GANIL. New neutron-rich isotopes,  $^{34}\text{Ne}$  and  $^{37}\text{Na}$ , have been observed together with some evidence for the particle instability of  $^{33}\text{Ne}$  and  $^{36}\text{Na}$ .

Recent data on mass measurements of neutron-rich nuclei at GANIL and some characteristics of binding energies in this region are discussed. Nuclear binding energies are very sensitive to the existence of nuclear shells and together with the measurements of instability of double magic nuclide  $^{28}\text{O}$  they provide information on changes in neutron shell closures of very neutron-rich isotopes from carbon up to calcium. The conclusion about rearrangements in neutron shell closures is given.

The spectroscopic measurements can reveal details of the underlying microscopic structures, the in-beam  $\gamma$ -ray spectroscopy is an effective tool to check for shell closures. This result of the  $\gamma$ -ray energies of the first  $2^+$  level for even-even nuclei for  $N$  in the range 12–32 is discussed.

The investigation has been performed at the Flerov Laboratory of Nuclear Reactions, JINR.

Preprint of the Joint Institute for Nuclear Research. Dubna, 2002

Макет *Т. Е. Попеко*

Подписано в печать 05.11.2002.

Формат 60 × 90/16. Бумага офсетная. Печать офсетная.

Усл. печ. л. 1,18. Уч.-изд. л. 1,6. Тираж 300 экз. Заказ № 53604.

Издательский отдел Объединенного института ядерных исследований  
141980, г. Дубна, Московская обл., ул. Жолио-Кюри, 6.

E-mail: [publish@pds.jinr.ru](mailto:publish@pds.jinr.ru)

[www.jinr.ru/publish](http://www.jinr.ru/publish)